

**High Yield Production of Inorganic Graphene-Like  
Materials (MoS<sub>2</sub>, WS<sub>2</sub>, BN) Through Liquid Exfoliation  
Testing Key Parameters**

by

Fei Pu

Submitted to the Department of Materials  
Science and Engineering in Partial  
Fulfillment of the Requirements for the  
Degree of

Bachelor of Science

at the

Massachusetts Institute of Technology

May 2012

© 2012 Fei Pu  
All rights reserved

The author hereby grants to MIT permission to reproduce and to  
distribute publicly paper and electronic copies of this thesis document in whole or in part  
in any medium now known or hereafter created.

Signature of Author .....  
Department of Materials Science and Engineering  
May 15, 2012

Certified by .....  
Linn W. Hobbs  
Professor of Material Science and Nuclear Engineering, Thesis Supervisor

Accepted by .....  
Jeffrey Grossman  
Carl Richard Soderberg Associate Professor of Power Engineering  
Chair, Undergraduate Thesis Committee

# **High Yield Production of Inorganic Graphene-Like Materials (MoS<sub>2</sub>, WS<sub>2</sub>, BN) Through Liquid Exfoliation Testing Key Parameters**

By

Fei Pu

Submitted to the Department of Materials Science and Engineering  
on May 15, 2012  
in Partial Fulfillment of the Requirements for the Degree of  
Bachelor of Science

## **Abstract**

Inorganic graphene-like materials such as molybdenum disulfide (MoS<sub>2</sub>), tungsten sulfide (WS<sub>2</sub>), and boron nitride (BN) are known to have electronic properties. When exfoliated into layers and casted onto carbon nanofilms, they can become potentially cheap and efficient electronic materials for magnetic sensing and energy storage devices. The goal of this experiment is to use a general liquid-phase method to exfoliate and optimize a number of parameters that can yield the highest concentration of layered quantities of MoS<sub>2</sub>, WS<sub>2</sub>, and BN. The key parameters optimized were material concentration, surfactant concentration, sonication method and duration, and centrifuge speed. Therefore, different concentrations of the three materials were mixed with different concentrations of the surfactant, sodium cholate hydrate (C<sub>24</sub>H<sub>39</sub>NaO<sub>5</sub> · xH<sub>2</sub>O), to make suspensions. These suspensions were then sonicated and centrifuged at different durations and speeds, respectively. Absorption was measured for all of the suspensions using ultraviolet-visible spectrometer to determine what parameters yielded the highest concentration of the three materials since a high UV absorption generally equated to a high yield of the layered materials. The final optimal parameters that yielded the highest concentration of each material were: 3 mg/ml material concentration, 3 mg/ml surfactant concentration, 30-minute continuous tip sonication method, and 1-hr 500 RPM centrifugation. Droplets of these optimal suspensions were then casted onto carbon nanofilms, and transmission electron microscopy (TEM) was performed on the films to confirm the layered, flaked characteristics and the hexagonal structures of MoS<sub>2</sub>, WS<sub>2</sub>, and BN.

# Table of Contents

<b>LIST OF FIGURES</b>	5
<b>LIST OF TABLES</b>	7
<b>ACKNOWLEDGEMENTS</b>	8
<b>1. INTRODUCTION</b>	
1.1 Graphene and its fabrication challenges	9
1.2 Graphene sheets through liquid exfoliation	10
1.3 Inorganic graphene-like materials (MoS <sub>2</sub> , WS <sub>2</sub> , BN)	11
1.3.1 Molybdenum disulfide (MoS <sub>2</sub> ) and tungsten disulfide (WS <sub>2</sub> )	12
1.3.2 Boron Nitride (BN)	13
1.4 Making MoS <sub>2</sub> , WS <sub>2</sub> , BN sheets through liquid exfoliation	13
1.5 Methodology and theory of experiment	14
1.5.1 Key parameters	14
1.5.2 Assessment methods	14
<b>2. EXPERIMENTAL PROCEDURES</b>	
2.1 Chemicals and equipment	15
2.2 General methods	16
2.3 Optimization steps	17
2.3.1 Step 1: Sonification method	17
2.3.2 Step 2: Sonification duration	17
2.3.3 Step 3: Surfactant concentration	17
2.3.4 Step 4: Material concentration	18
2.3.5 Step 5: Centrifuge speed	18
<b>3. RESULTS &amp; DISCUSSION</b>	

3.1	Results and discussion of the optimization process	18
3.1.1	<i>Step 1: Optimizing sonication method</i>	18
3.1.2	<i>Step 2: Optimizing the duration of sonication tip method</i>	21
3.1.3	<i>Step 3: Optimizing surfactant concentration</i>	23
3.1.4	<i>Step 4: Optimizing material concentration</i>	26
3.1.5	<i>Step 5: Optimizing centrifuge speed</i>	29
3.1.6	<i>Final optimized parameters in yielding highest absorption</i>	33
3.1.7	<i>Finding concentration with absorptivity <math>\alpha</math></i>	33
3.1.8	<i>Optimal concentration of each material</i>	34
3.2	Results and discussion of the TEM images	35
<b>4.</b>	<b>CONCLUSION</b>	39
<b>5.</b>	<b>FUTURE STUDY &amp; LIMITATIONS</b>	40
<b>6.</b>	<b>REFERENCES</b>	41

## List of Figures

- Figure 1.** Honey-comb lattice and dark shiny appearance of graphene.
- Figure 2.** Stacked three-layer hexagonal structure of MoS<sub>2</sub>.
- Figure 3.** Stacked three-layer hexagonal structure of BN.
- Figure 4a.** Suspensions after sonication by tip or bath method for 30 minutes.
- Figure 4b.** Absorption for MoS<sub>2</sub> comparing sonication by tip and bath dispersion methods for 30 minutes.
- Figure 4c.** Absorption for WS<sub>2</sub> comparing sonication by tip and bath dispersion methods for 30 minutes.
- Figure 4d.** Absorption for BN comparing sonication by tip and bath dispersion methods for 30 minutes.
- Figure 5a.** Suspensions after sonication by tip method for different durations.
- Figure 5b.** Absorption for MoS<sub>2</sub> after sonication by tip method for different durations.
- Figure 5c.** Absorption for WS<sub>2</sub> after sonication by tip method for different durations.
- Figure 5d.** Absorption for BN after sonication by tip method for different durations.
- Figure 6a.** Suspensions with a fixed material concentration (1gm/ml) and different surfactant concentrations (1 mg/ml, 3 mg/ml, and 5 mg/ml).
- Figure 6b.** Absorption for MoS<sub>2</sub> (1mg/ml) with different concentration of surfactant.
- Figure 6c.** Absorption for WS<sub>2</sub> (1mg/ml) with different concentration of surfactant.
- Figure 6d.** Absorption for BN (1mg/ml) with different concentration of surfactant.
- Figure 7a.** Samples with fixed surfactant(3gm/ml) and different concentration of material(0.1 mg/ml, 1 mg/ml, 3 mg/ml, and 5 mg/ml).
- Figure 7b.** Absorption for different concentrations of MoS<sub>2</sub> with fixed surfactant (3mg/ml).
- Figure 7c.** Absorption for different concentrations of WS<sub>2</sub> with fixed surfactant (3mg/ml).
- Figure 7d.** Absorption for different concentrations of BN with fixed surfactant (3mg/ml).

- Figure 8a.** Suspensions centrifuged at different speeds (in RPM).
- Figure 8b.** Absorption for MoS<sub>2</sub> after being centrifuged at different speeds (in RPM).
- Figure 8c.** Absorption for WS<sub>2</sub> after being centrifuged at different speeds (in RPM).
- Figure 8d.** Absorption for BN after being centrifuged at different speeds (in RPM).
- Figure 9a.** TEM images showing the layered and flaked characteristics of exfoliated MoS<sub>2</sub>.
- Figure 9b.** Diffraction pattern reveals the hexagonal structure of exfoliated MoS<sub>2</sub>.
- Figure 10a.** TEM images showing the layered and flaked characteristics of exfoliated WS<sub>2</sub>.
- Figure 10b.** Diffraction pattern reveals the hexagonal structure of exfoliated WS<sub>2</sub>.
- Figure 11a.** TEM images showing the layered and flaked characteristics of exfoliated BN.
- Figure 11b.** Diffraction pattern reveals the hexagonal structure of exfoliated BN.

## List of Tables

- Table 1.** Parameters measured for deducing the relationship between absorption and material concentration for each material.
- Table 2.** Final optimal concentration of each material after the supernatant was removed from the suspensions.

# Acknowledgements

This work would not have been possible without the help, guidance, and support of many individuals, whom I would like to thank sincerely.

First, I would like to thank Professor Hobbs in guiding and helping my thesis work. His patience and teaching were invaluable. Also, I cannot express my sincere gratitude for his kindness, advice, and constant support as my mentor and advisor in the past few years at MIT. I consider myself very lucky for having had the opportunity to be his student.

In addition, I would like to thank Dr. Valeria Nicolosi, who has allowed me to part of her lab and research project at University of Oxford. She has given me the precious opportunity to delve into my research interests. I appreciated her guidance and valuable advice throughout the entire research process.

Finally, I would like to thank my family, in particular my mother, father, and sister, Jue, who have always been willing to support and believe me in my endeavors. And I would like to thank my beloved Leo, who has always been there for me, providing care and giving encouragements.



# 1. Introduction

## 1.1 Graphene and its fabrication challenges

Graphene, with one-atom-thick planar sheets of  $sp^2$ -bonded carbon in hexagonal structure, has a densely packed two-dimensional (2D) honeycomb lattice and dark shiny appearance, as shown in Figure 1.<sup>[1]</sup> Because of its unique layer-form structure, it has been known to have attractive electronic properties such as high electrical conductivity with little resistance or heat generation. The layered form and array structure of graphenes make them ideal materials for high speed transistors or integrated circuits that consume less energy than conventional silicon electronics.<sup>[1]</sup>

Successful dispersion of graphene into layers enables the use of low-cost suspension processing techniques to fabricate various potentially useful graphene-like materials, which have superior physical and material properties. Due to their symmetry, low weight to surface ratio, and high porosity, nanofilms coated with thin layers of inorganic graphene-like materials have potential applications from ultralight anti-corrosive materials to electron field emitters.<sup>[2]</sup> In addition, the semiconducting properties make the inorganic nanofilms potential materials for further miniaturization of optoelectronic materials. Finally, the hexagonal structure of graphene-like materials make them possible applications in non-linear optics and solar technology because these conducting nanofilms can detect self-inductance and resistance quickly and efficiently. For example, applications range from the sharp tips in scanning spectroscopy probes to other magnetic, electronic detecting devices.<sup>[3]</sup>

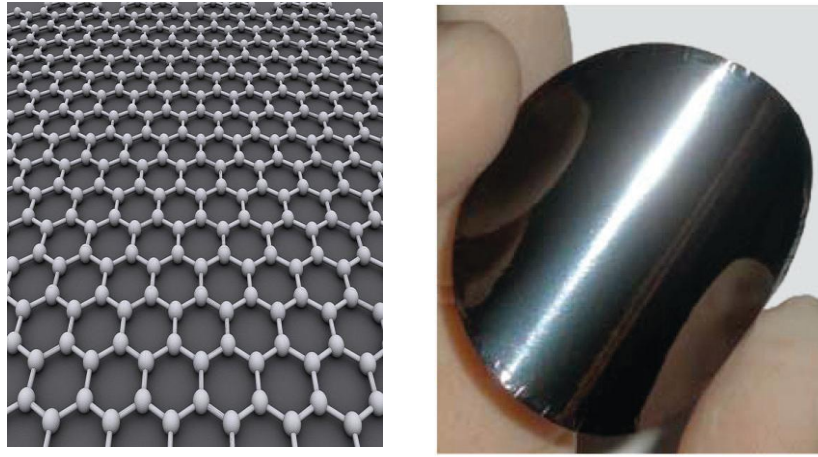


**Figure 1.** Honey-comb lattice structure and dark shiny appearance of graphene.<sup>[1]</sup>

Yet the challenge lies in the production of thin graphene layers because the process of separating graphene into separate, defined layers can be difficult.<sup>[3]</sup> Traditionally graphene sheets are made by micromechanical cleavage, epitaxial growth, and bottom-up organic synthesis.<sup>[3]</sup> These processes all follow the similar procedure of peeling layers graphite crystals. In all of these synthesis routes, keeping the graphene sheets individually separated is the most important and challenging part. Bulk graphene sheets, if left unprotected, will spontaneously agglomerate and even restack to form graphite. Also, the yield is very low, which makes the production process an expensive one.

## **1.2 Graphene sheets through liquid exfoliation**

It was not until 2004 that physicists at the University of Manchester and the Institute for Microelectronics Technology were able to first isolate individual graphene planes using adhesive tape to obtain flakes that exhibited unique electronic properties.<sup>[4]</sup> The discovery has led to a great interest in the science community to study large-scale production graphene sheets.

Now, the most common method discovered to produce layers of graphene is through chemical, or liquid exfoliation, of graphene oxide whereby graphite oxide is dispersed with surfactants in water suspensions to break up graphite oxide into particle aggregates to produce layers of 2D crystals of graphene oxide.<sup>[4]</sup> Subsequent deoxygenation through chemical reduction can transform the insulating graphene oxide to conductive graphene. Many researchers focus on graphite oxide instead of graphite because the former is hydrophilic and has a larger interlayer distance. Thus, it was easier to exfoliate graphite oxide than graphite.<sup>[4]</sup> However, this technique has one significant disadvantage. The oxidation process introduces structural defects in the graphene sheets as evidenced by Raman spectroscopy.<sup>[4]</sup>

A breakthrough method has been developed, in which graphite is directly exfoliated by dispersing it into certain surfactant suspensions.<sup>[6]</sup> In general, exfoliation can only occur when the net energetic cost is very small. So the underlying phenomenon depends on the fact that certain surfactant suspensions have surface energy that matches so well with graphene that exfoliation occurs naturally when dispersed together. Such method is non-oxidative, so no defects are introduced on the final graphene sheets. TEM analysis shows that the vacuum filtered flakes of the dispersed suspensions on nanofilms are in monolayers and have few defects.<sup>[5]</sup>

### **1.3 Inorganic graphene-like materials (MoS<sub>2</sub>, WS<sub>2</sub>, BN)**

While graphene is the most studied monolayer material, layered inorganic graphene-like materials, such as molybdenum disulfide (MoS<sub>2</sub>), tungsten sulfide (WS<sub>2</sub>),

and boron nitride (BN) have also shown to display similar material properties as graphene and can be used for electronic sensing and energy storage applications.

### ***1.3.1 Molybdenum disulfide (MoS<sub>2</sub>) and tungsten disulfide (WS<sub>2</sub>)***

MoS<sub>2</sub> and WS<sub>2</sub> are both black inorganic layered material with structure similar to that of graphene. They are related because both can be classified as transition metal dichalcogenides (TMDs) with the chemical formula of MX<sub>2</sub>. TMDs generally consist of hexagonal layers of metal atoms, M, sandwiched between two layers of chalcogen atoms, X. [1] While the bonding of the tri-layers is covalent, adjacent sheets are bonded via Van der Waals interactions to form a 3D crystal. There are currently 40 different types of combination of TMDs with different chalcogen atoms. Depending on the co-ordination and oxidation state of the metal atoms, TMDs can be metallic, semi-metallic or semiconducting. MoS<sub>2</sub> and WS<sub>2</sub> are semiconductors with superconductivity and charge wave effects that make them versatile for useful electronic materials. Figure 2 shows the stacked three-layer hexagonal structure of MoS<sub>2</sub> with a layer of molybdenum (Mo) inserted in between every two layers of sulfur (S). WS<sub>2</sub> has very similar structure, with tungsten(W) replacing Mo. [1]

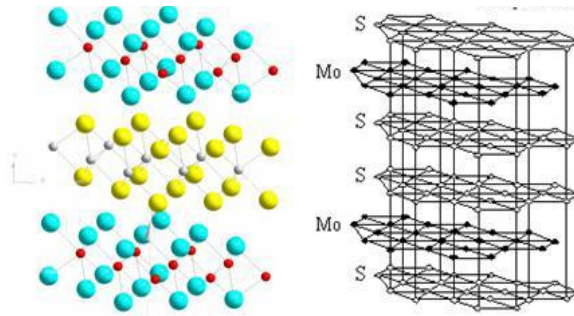


**Figure 2.** Stacked three-layer hexagonal structure of MoS<sub>2</sub>. [1]

### 1.3.2 Boron Nitride (BN)

Boron nitride is a white-colored crystal that has the same structure as graphite except for the substitution of the carbon atoms by boron and nitrogen atoms. Like MoS<sub>2</sub> and WS<sub>2</sub>, it also has a hexagonal structure displaced in layers as shown below in **Figure 3**.

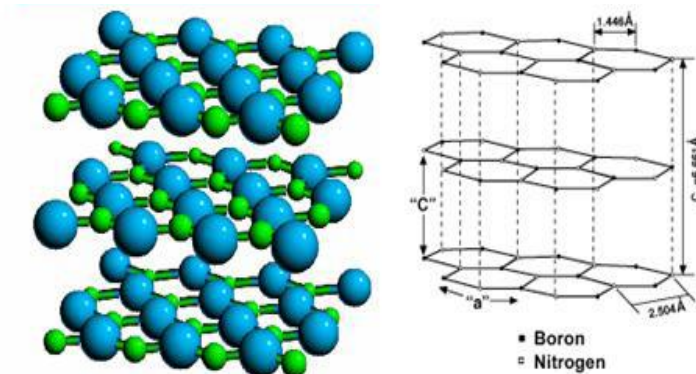


**Figure 3.** Stacked three-layer hexagonal structure of BN. <sup>[1]</sup>

Because of excellent thermal and chemical stability, boron nitride ceramics are traditionally used as parts of high-temperature equipment. Unlike MoS<sub>2</sub> and WS<sub>2</sub>, both of which are semiconductors, BN is an electrical insulator with a wide bandgap of ~5.5 eV. <sup>[5]</sup>

### 1.4 Making MoS<sub>2</sub>, WS<sub>2</sub>, and BN sheets through liquid exfoliation

All three materials (MoS<sub>2</sub>, WS<sub>2</sub>, BN) in layered form exhibit useful electronic properties. Yet, they have not been widely produced because of the difficulty in exfoliating them into mono or few-layer flakes in large quantities. <sup>[4]</sup>

Just as graphite, liquid exfoliation has been introduced as the optimal method to exfoliate the three materials into mono- or few-layers.<sup>[4]</sup> The method can produce layered flakes for large production. Similar to the process of exfoliating graphite, MoS<sub>2</sub>, WS<sub>2</sub>, BN powders are dispersed with a compatible surfactant that has matching surface energy with the material so that exfoliation occurs naturally.<sup>[6]</sup> In recent studies, the liquid exfoliation procedure has been performed on MoS<sub>2</sub>, WS<sub>2</sub>, and BN. Transmission electron microscopy (TEM) analysis also confirmed that both mono and few-layered flakes were formed.

## **1.5 Methodology and theory of experiment**

In this experiment, the production of layering MoS<sub>2</sub>, WS<sub>2</sub>, and BN is not studied because the method for doing so has already been developed. Instead, the project focuses on optimizing each step of the liquid exfoliation process.

### ***1.5.1 Key parameters***

The four key parameters tested are 1) material concentration, 2) surfactant concentration, 3) sonification method and duration, and 4) centrifuge speed. By varying and testing these four key parameters, the goal is to ultimately decide 1) the optimal concentration of each of the three materials, 2) the optimal concentration of the surfactant, 3) the optimal method of sonication, and the 4) optimal centrifuge speed to yield the highest concentration of each material.

### ***1.5.2 Assessment methods***

To measure the concentration of each material, UV-visible spectrophotometry (UV-Vis NIR) is used. Molecules in suspension absorb ultraviolet or visible light. The absorption of a suspension increases as attenuation of the beam increases. Thus, absorption,  $A$ , is directly proportional to the path length,  $L$ , and the concentration,  $C$ , of the absorbing species, as formalized in *Beer's Law* in Equation 1

$$A = \alpha CL \quad \text{Equation (1)}$$

where  $\alpha$  is the absorptivity. The absorption is measured for all suspensions in the wavelength range between 400 and 1200 nm.

To examine if the exfoliation process affected the structure of each material and that exfoliated suspensions contained layers, transmission electron microscopy (TEM) was used to confirm the results. TEM images were recorded to ascertain the hexagonal structure of the materials and whether the exfoliated suspensions of each material contained layered flakes.

## **2. Experimental Procedures**

### **2.1 Chemicals and equipment**

The  $\text{WS}_2$  and  $\text{MoS}_2 < 2\mu$ , 99% powders were purchased from Adrich Chemistry. BN powder  $< 2\mu$ , 99% was purchased from Saint-Gobain Ceramics. Surfactant sodium cholate hydrate ( $\text{C}_{24}\text{H}_{39}\text{NaO}_5 \cdot x\text{H}_2\text{O}$ ) powder was purchased from Sigma Ultra. The UV-

Vis/NIR spectrometer used was a Cary 5000 model purchased from Varian Inc. The centrifuge used was the Microfuge model purchased from Sigma Centrifuges. The sonication bath used was an industrial bath, model U1250, purchased from Ultrawave Ultrasonic. The sonication tip processor used was the UP100H Ultrasonic Processor model purchased from Hielscher Ultrasound Technology. Lastly, the TEM used was a JEOL 2100 instrument.

## **2.2 General methods**

Stock surfactant, sodium cholate hydrate, solutions of different concentrations of 1mg/ml, 3 mg/ml, and 5 mg/ml were prepared with distilled water and stirred overnight by magnetic stirrer. Material ( $WS_2$  MoS<sub>2</sub>, BN) suspensions of different concentrations of 0.1 mg/ml, 1 mg/ml, 3 mg/ml, and 5 mg/ml were prepared with distilled water. Different concentrations of the surfactant solutions and material suspensions were then mixed and filled into 10 mL cylindrical vials. These vial suspensions were then dispersed using sonication bath method for 1 hour or sonication tip method for periods of 2 minutes, 30 pulsed minutes, and 30 minutes. After sonication, the vial suspensions were then centrifuged for 60 minutes with different speeds of 500, 1500, 3000, and 5000 RPM. After centrifugation, the supernatant or top 5 ml of clear liquid of each suspension was decanted into a new cuvette in order to prepare for UV-Vis/NIR spectrometer. Absorptions were measured and later plotted and analyzed to discover which parameters yielded the highest absorption. To relate absorption to concentration, the absorptivity  $\alpha$  was found. At last, a few millimeters of the optimal material suspensions with the highest concentration were dispersed on meshed circular carbon nanotube films (400-mesh).



TEM was performed on the films to confirm the layered, flaked characteristics of the exfoliated materials.

### **2.3 Optimization steps**

With this general experimental setup in place, the optimization steps carried out were as follows. These steps were carried out chronologically in order to waste the least amount of time in optimizing absorption, or concentration, of the suspensions.

#### ***2.3.1 Step 1: Sonication method***

Surfactant concentration, material concentration, and centrifuge speed were held constant at first. The sonication method (either bath or tip) was changed to see which sonication method was better in dispersing the suspensions. The method that optimized absorption for each material suspension was chosen and used for later suspensions.

#### ***2.3.2 Step 2: Sonication duration***

Again, surfactant concentration, material concentration, and centrifuge speed were held constant. This time, the duration of the sonication method was changed to see how it affected absorption. The duration that optimized the absorption for each material suspension was chosen and used for later suspensions.

#### ***2.3.3 Step 3: Surfactant concentration***

For this step, the sonication method and duration were fixed. The material concentration and the centrifuge speed were held constant, but the surfactant

concentration was changed. The surfactant concentration level that optimized absorption for each material suspension was chosen and used for later suspensions.

#### ***2.3.4 Step 4: Material concentration***

For this step, the sonication method and duration were fixed. The surfactant concentration and centrifuge speed was held constant, but the material concentration was changed. The material concentration level that optimized absorption for each material suspension was chosen and used for later suspensions.

#### ***2.3.5 Step 5: Centrifuge speed***

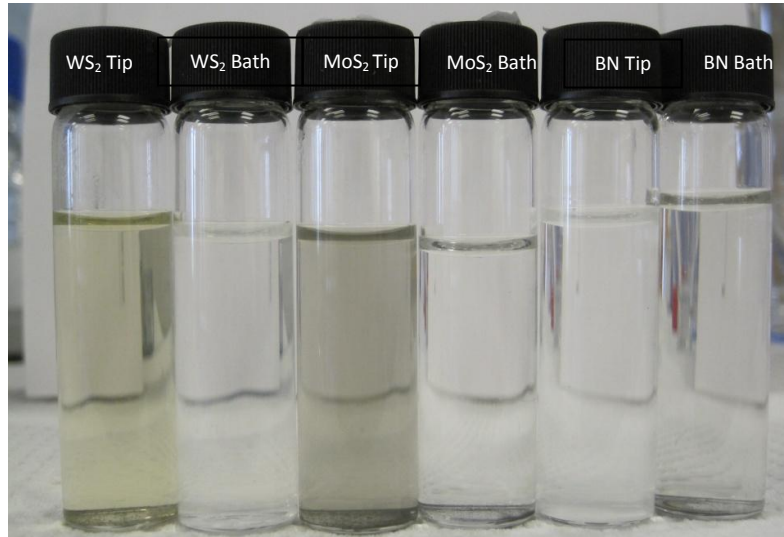
Lastly, all parameters except for the centrifuge speed were fixed. The centrifuge speed was changed. The centrifuge speed that optimized absorption was chosen. All parameters were tested and optimized. TEM was performed on carbon nanofilms, which were dispersed with optimal suspensions, to confirm results.

### **3. Results & Discussion**

#### **3.1 Results and discussion of the optimization process**

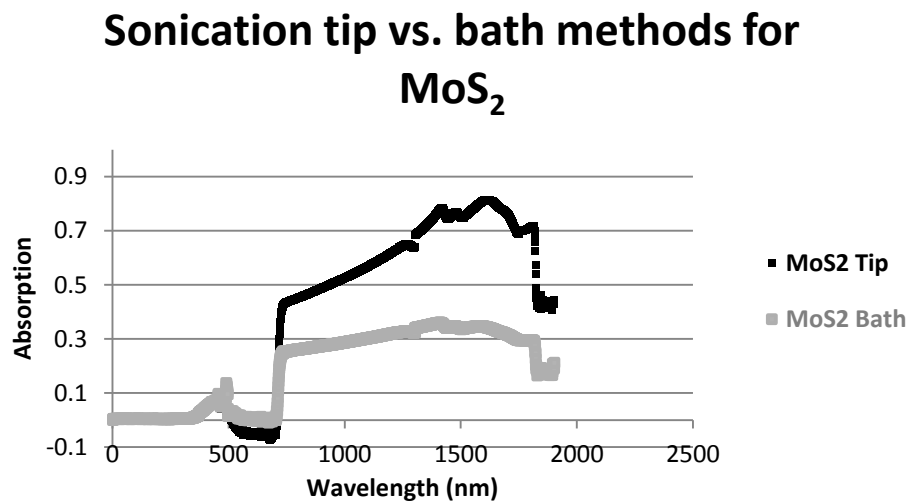
##### ***3.1.1 .1 Step 1: Optimizing the sonication method***

MoS<sub>2</sub>, WS<sub>2</sub>, and BN powders of 1mg/ml concentration were mixed with the surfactant of 1mg/ml concentration to make 10 mL suspensions. Then, these suspensions were sonicated either by tip or bath method for 30 minutes. Lastly, they were centrifuged for 60 minutes with a fixed RPM of 500. Absorption was measured using UV-Vis/NIR spectrometer, and figures 4a-4d show the suspensions and the absorption curves for all three materials.



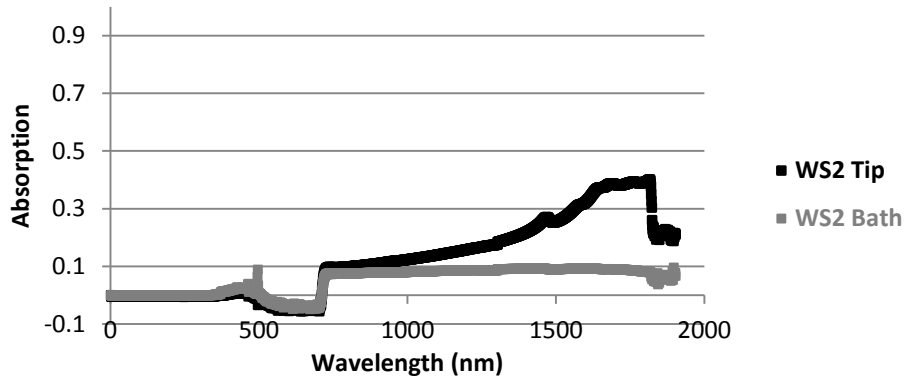
**Figure 4a.** Suspensions after sonication by tip or bath method for 30 minutes.

Figure 4a shows that the sonication tip method yielded a more homogenous and darker suspension for all of the three materials, while the sonication bath method left the suspensions unchanged. Figures 4b-4d quantify this qualitative observation with sonication tip method yielding a higher absorption curve.



**Figure 4b.** Absorption for MoS<sub>2</sub> comparing sonication by tip and bath dispersion methods for 30 minutes.

### Sonication tip vs. bath methods for WS<sub>2</sub>



**Figure 4c.** Absorption for WS<sub>2</sub> comparing sonication by tip and bath dispersion methods for 30 minutes.

### Sonication tip vs. bath methods for BN

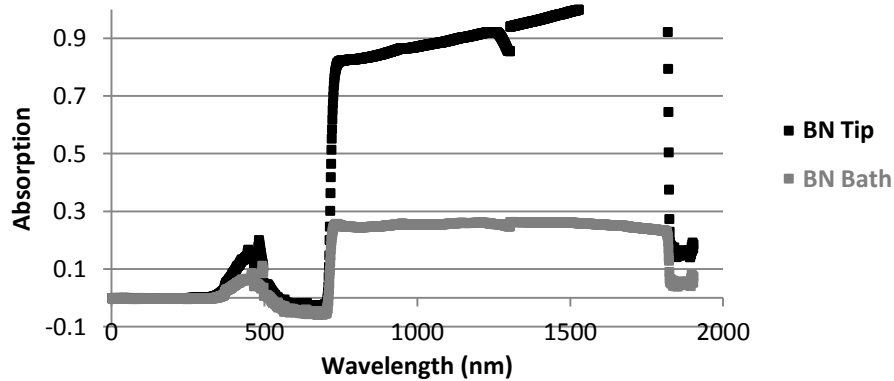
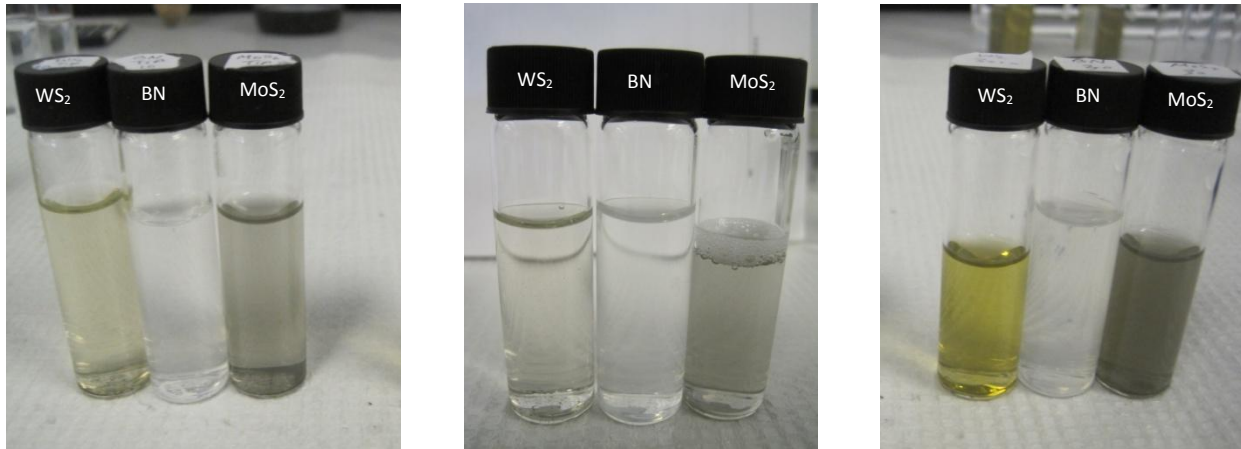


**Figure 4d.** Absorption for BN comparing sonication by tip and bath dispersion methods for 30 minutes.

For all three materials, it was evident that the sonication tip method yielded higher absorptions for 400 to 1200 nm wavelengths. After step-1 optimization, the sonication dispersion bath method was eliminated. For the remaining steps, the sonication tip dispersion method was used.

### 3.1.2 Step 2: Optimizing the duration of sonication tip dispersion method

MoS<sub>2</sub>, WS<sub>2</sub>, and BN of 1mg/ml concentration were mixed with the surfactant of 1mg/ml concentration to make 10 mL suspensions. These suspensions were then sonicated by tip only, but for three different durations: 2 minute continuous, 30 minute pulsed, and 30 minute continuous. Lastly, they were centrifuged for 60 minutes with a fixed RPM of 500. Absorption was measured using UV-Vis/NIR spectrometer, and figures 5a-5d show the suspensions and the absorption curves for all three materials.



2 min continuous tip

30 min pulsed tip

30 min continuous tip

**Figure 5a.** Suspensions after sonication by tip method for different durations.

From figure 5a, the 30 minute continuous sonication tip method yielded the darkest suspension, translating to the highest absorption.

## Varying sonication tip duration for MoS<sub>2</sub>

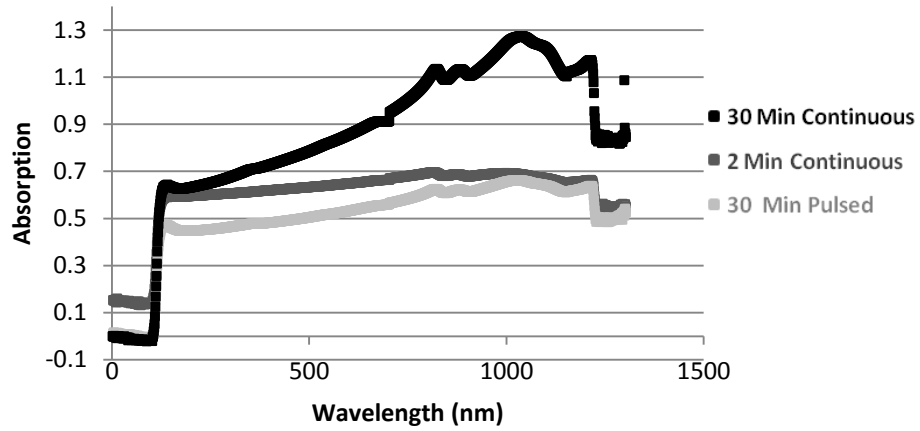


**Figure 5b.** Absorption for MoS<sub>2</sub> after sonication by tip method for different durations.

## Varying sonication tip duration for WS<sub>2</sub>

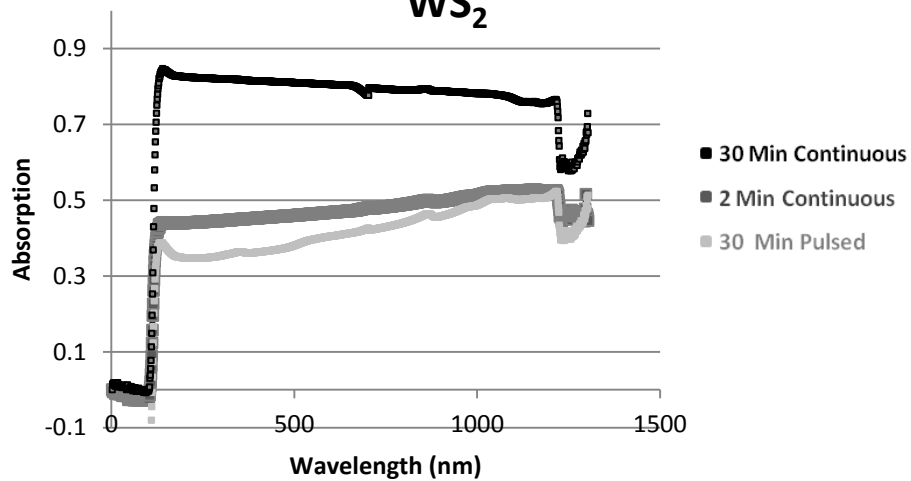


**Figure 5c.** Absorption for WS<sub>2</sub> after sonication by tip method for different durations.

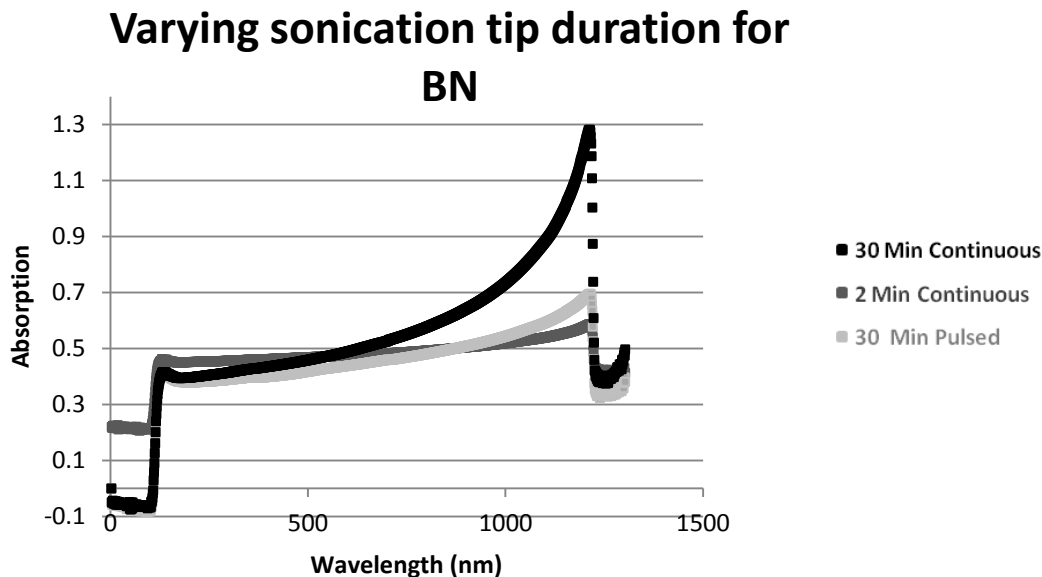


**Figure 5d.** Absorption for BN after sonication by tip method for different durations.

For all three materials, it was evident that the sonication tip method for 30 minutes yielded the highest absorption for 400 to 1200 nm wavelengths. After step 2 optimization, the 2-minute continuous and 30-minute pulsed durations were eliminated. For the remaining steps, the sonication tip method for 30 continuous minutes was used.

### ***3.1.3 Step 3: Optimizing surfactant concentration***

MoS<sub>2</sub>, WS<sub>2</sub>, and BN powders of 1mg/ml concentration were mixed with three different concentrations of 1 mg/ml, 3 mg/ml, and 5 mg/ml to make 10 mL suspensions. Then, these suspensions were sonicated by tip for 30 continuous minutes. Lastly, they were centrifuged for 60 minutes with a fixed RPM of 500. Absorption was measured using UV-Vis/NIR spectrometer, and figures 6a-6d show the suspensions and the absorption curves for all three materials.

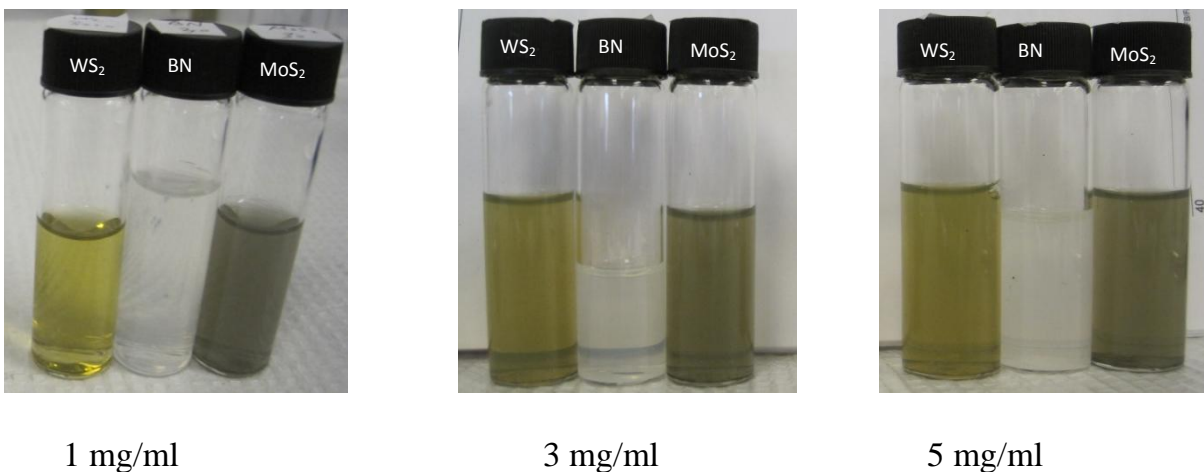


**Figure 6a.** Suspensions with a fixed material concentration (1gm/ml) and different surfactant concentrations (1 mg/ml, 3 mg/ml, and 5 mg/ml).

Figure 6a shows that suspensions of 3 mg/ml and 5 mg/ml surfactant concentrations were darker and more homogenous. Figures 6b-6d would reveal the corresponding absorption curves.

### Varying surfactant concentration with 1mg/ml MoS<sub>2</sub>

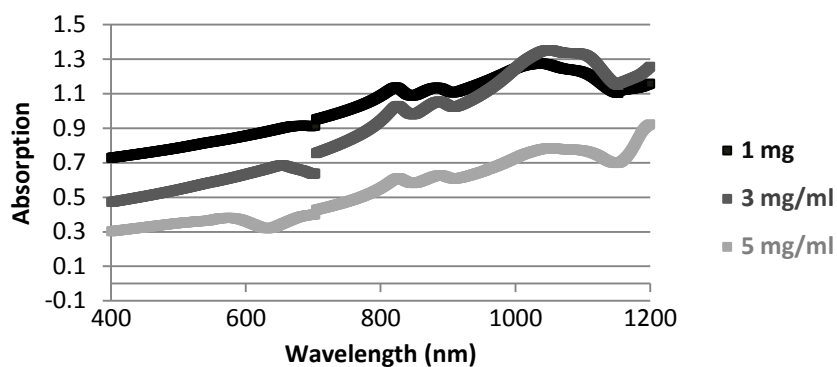


**Figure 6b.** Absorption for MoS<sub>2</sub> (1mg/ml) with different concentration of surfactant.



### Varying surfactant concentration with 1mg/ml WS<sub>2</sub>

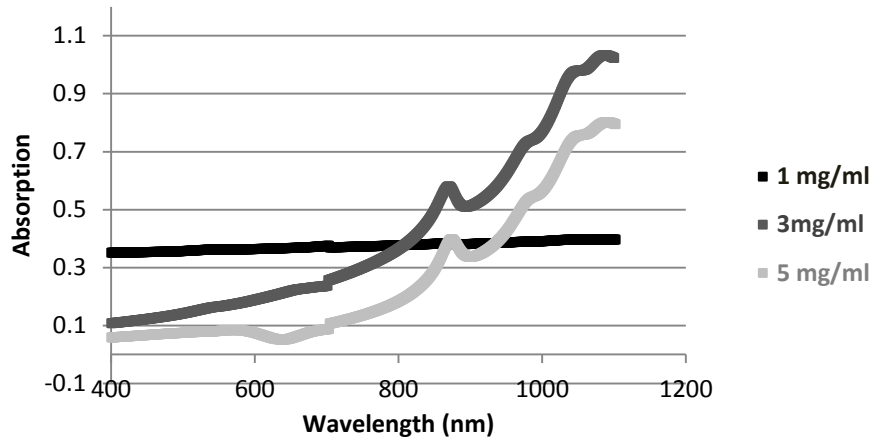


**Figure 6c.** Absorption for WS<sub>2</sub> (1mg/ml) with different concentration of surfactant.

### Varying surfactant concentration with 1mg/ml BN

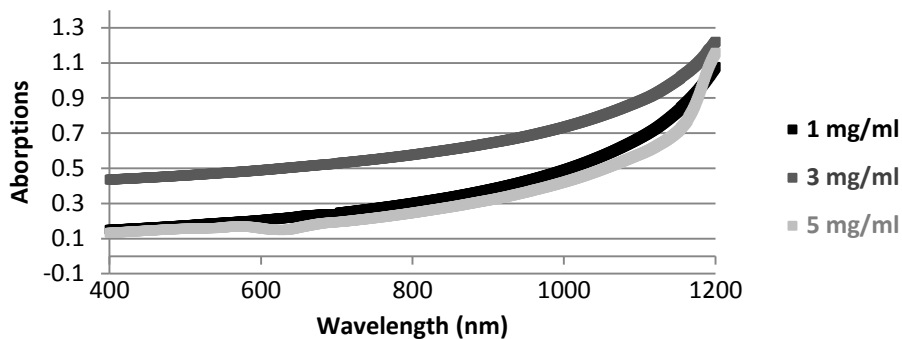


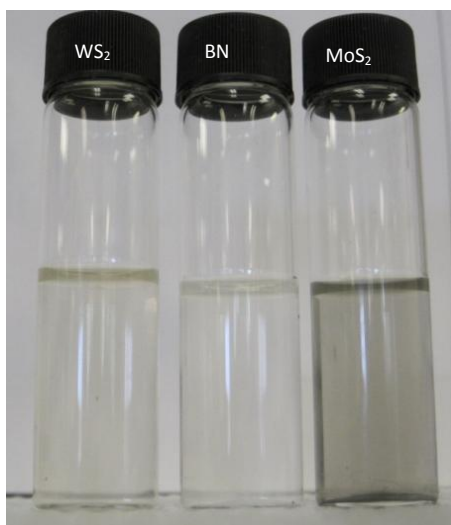
**Figure 6d.** Absorption for BN (1mg/ml) with different concentration of surfactant.

For all three materials, it was evident that a surfactant concentration of 3 mg/ml yielded the highest absorption for 400 to 1200 nm wavelengths. After step-

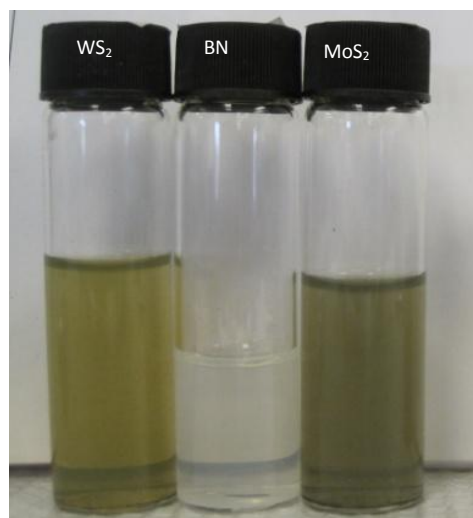
3 optimization, surfactant concentrations of 1 mg/ml and 5 mg/ml were eliminated. For the remaining optimization, a surfactant concentration of 3 mg/ml was used.

#### ***3.1.4 Step 4: Optimizing material concentration***

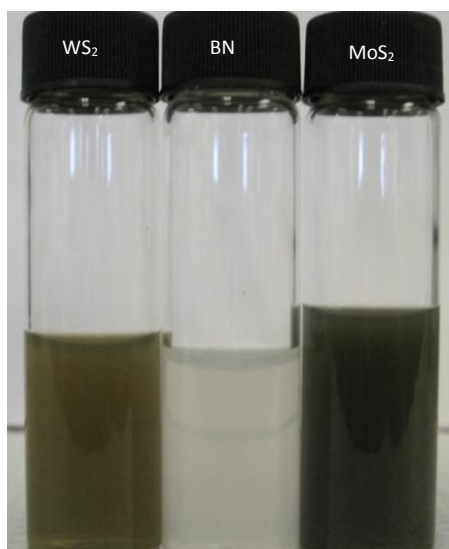
With the surfactant concentration of 3 mg/ml fixed, the concentrations of MoS<sub>2</sub>, WS<sub>2</sub>, and BN were varied (0.1 mg/ml, 1 mg/ml, 3 mg/ml, and 5 mg/ml) to make 10 mL suspensions. These suspensions were then sonicated by tip for 30 continuous minutes. Lastly, they were centrifuged for 60 minutes with a fixed RPM of 500. Absorption was measured using UV-Vis/NIR spectrometer, and figures 7a-7d show the suspensions and the absorption curves for all three materials.



0.1 mg/ml



1 mg/ml



3 mg/ml



5 mg/ml

**Figure 7a.** Samples with fixed surfactant (3gm/ml) and different concentration of material(0.1 mg/ml, 1 mg/ml, 3 mg/ml, and 5 mg/ml).

Figure 7a reveals that the 3 mg/ml suspensions were the darkest and the most homogenous. Figures 7b-7d confirm that 3 mg/ml material yielded the highest absorption. It is noted that the 5 mg/ml suspensions exceeded the optimal molar ratio of surfactant to material; thus, the suspensions appear as if they were not mixed at all.

### Varying MoS<sub>2</sub> material concentration with 3mg/ml surfactant

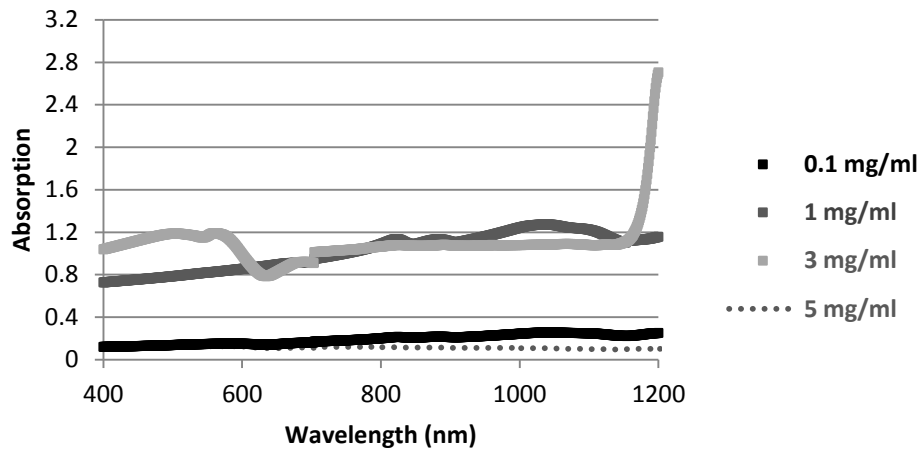


**Figure 7b.** Absorption for different concentrations of MoS<sub>2</sub> with fixed surfactant (3mg/ml).

### Varying WS<sub>2</sub> material concentration with 3mg/ml surfactant

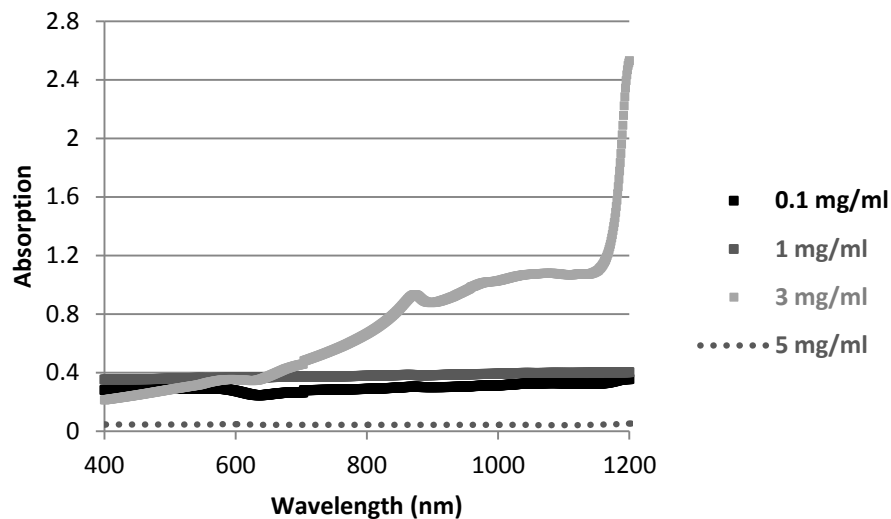


**Figure 7c.** Absorption for different concentrations of WS<sub>2</sub> with fixed surfactant (3mg/ml).

## Varying BN material concentration with 3mg/ml surfactant

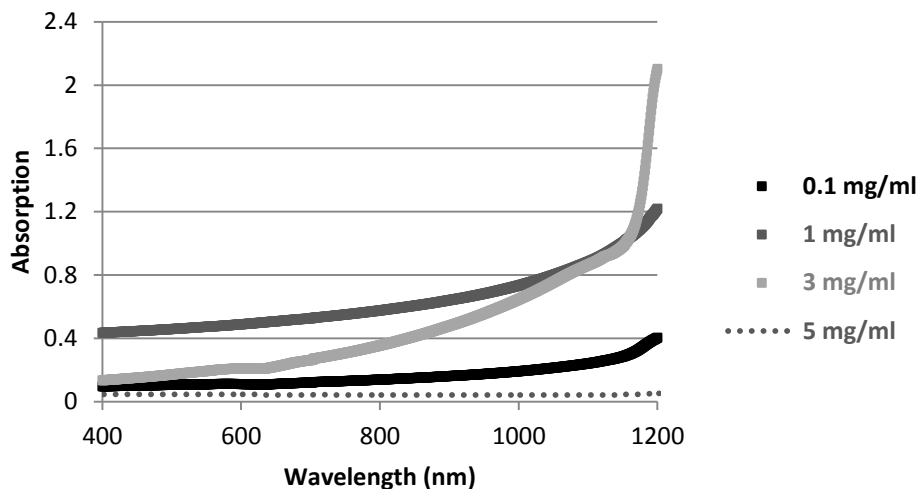


**Figure 7d.** Absorption for different concentrations of BN with fixed surfactant (3mg/ml).

On average, materials with a concentration of 3 mg/ml yielded the highest absorption for 400 to 1200 nm wavelengths, although the 1 mg/ml absorption curve was higher than 3 mg/ml absorption curve for BN. After step-4 optimization, material concentrations of 0.1 mg/ml, 1 mg/ml, and 5 mg/ml were eliminated. For the last step in optimizing centrifuge speed, a material concentration of 3 mg/ml was used.

### *3.1.5 Step 5: Optimizing centrifuge speed*

MoS<sub>2</sub>, WS<sub>2</sub>, and BN of 3mg/ml concentration were mixed with the surfactant of 3 mg/ml to make 10 mL suspension samples. Then, these suspensions were sonicated by tip method for 30 continuous minutes. Lastly, they were

centrifuged for 60 minutes with different speeds: 500 RPM, 1500 RPM, 3000 RPM, and 5000 RPM. Absorption was measured using UV-Vis/NIR spectrometer, and figures 8a-8d show the suspensions and the absorption curves for all three materials.



500 RPM



1500 RPM



3000 RPM



5000 RPM

**Figure 8a.** Suspensions centrifuged at different speeds (in RPM).

From figure 8a, a centrifugal speed of 500 RPM yielded the most homogenous and darkest suspensions. It could be hypothesized that a lower speed gave the samples more time and the right mixing environment for the surfactant and material to interact and form homogenous suspensions. Figures 8b-d confirm that a centrifuge speed of 500 RPM would yielded the highest absorption curve.

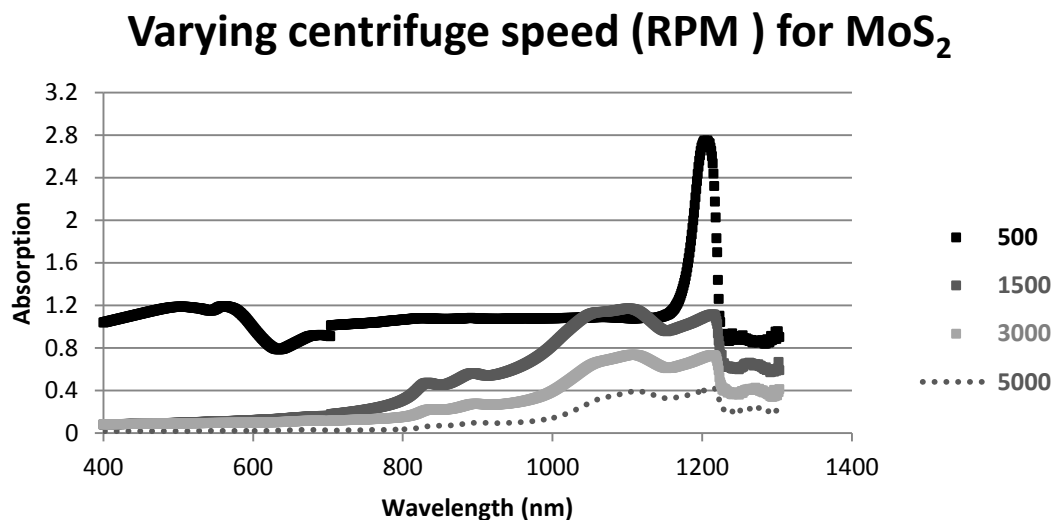


**Figure 8b.** Absorption for MoS<sub>2</sub> after being centrifuged at different speeds (in RPM).

### Varying centrifuge speed (RPM ) for WS<sub>2</sub>

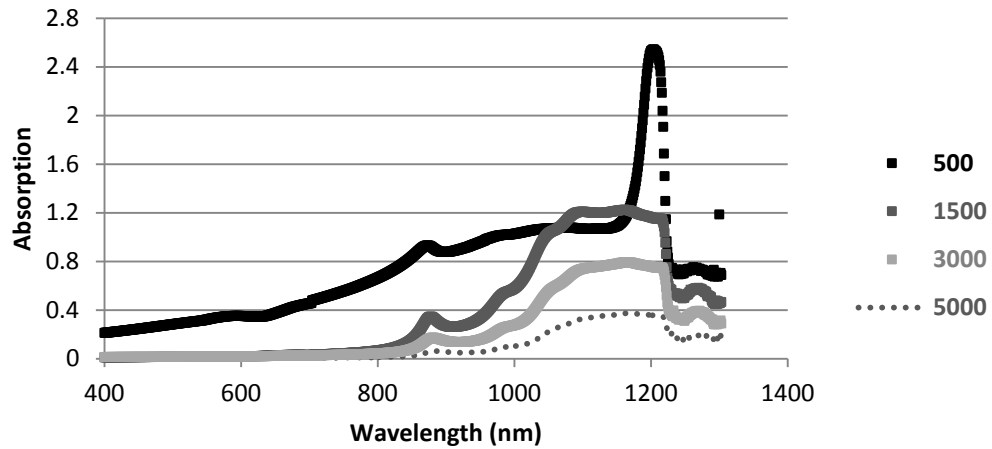


**Figure 8c.** Absorption for WS<sub>2</sub> after being centrifuged at different speeds (in RPM).

### Varying centrifuge speed (RPM ) for BN

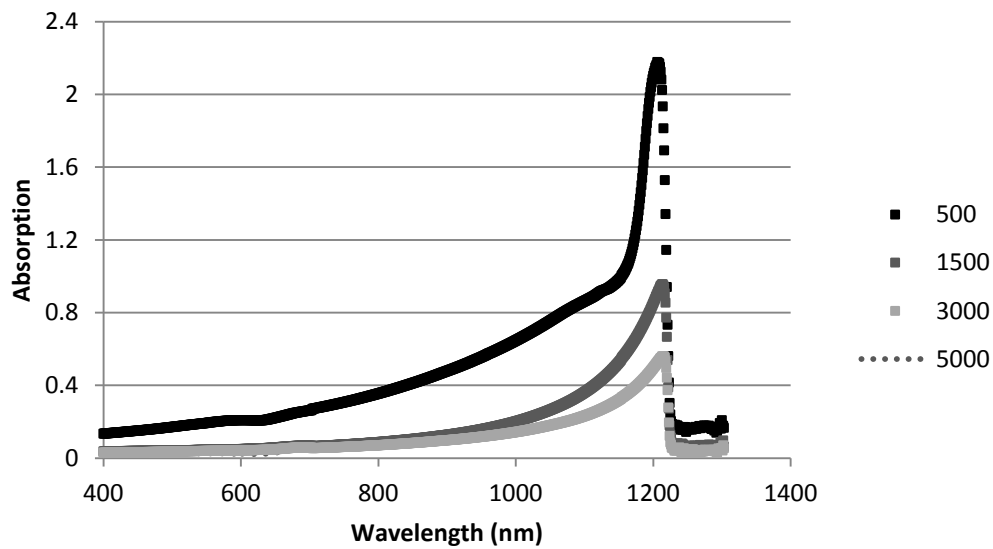


**Figure 8d.** Absorption for BN after being centrifuged at different speeds (in RPM).



For all three materials, it was evident that a RPM speed of 500 for 60 minutes yielded the highest absorption for 400 to 1200 nm wavelengths. Other speeds of 1500, 3000, and 5000 RPM were eliminated.

### ***3.1.6 Final optimized parameters in yielding the highest absorption***

The optimized parameters that yielded the highest absorption were: 30-minute continuous sonication tip method, 3 mg/ml surfactant concentration, 3 mg/ml material concentration, and 500 RPM centrifuge speed.

### ***3.1.7 Finding absorptivity, $\alpha$ , with absorption***

In all of the trials, absorption was used as the relative measure of concentration for the suspensions after the supernatant liquid was removed following centrifugation. In order to deduce the exact concentration of each material after centrifugation, the absorptivity  $\alpha$  must be found since concentration and absorption are related in Equation 2 through the Beer-Lambert's Law.

$$A = \alpha CL \qquad \text{Equation (2)}$$

$A$  was the absorption chosen at 640 nm.  $C$  was found by measuring the mass before and after sonication, centrifugation, and vacuum drying of each material over the initial 10 ml, 0.1 mg/ml suspensions.  $L = 100$  mm, which was the path length of the cuvette exposed to UV-Vis/NIR spectrometer. Table 1 summarizes the data used to deduce the absorptivity  $\alpha$  for each material.

**Table 1.** Parameters measured for deducing the relationship between absorption and material concentration for each material.

<b>Material</b>	<b>WS<sub>2</sub></b>	<b>MoS<sub>2</sub></b>	<b>BN</b>
<b>Mass before (mg)</b>	128.17	127.92	128.06
<b>Mass after (mg)</b>	128.76	129.64	129.04
<b>Mass difference (mg)</b>	0.59	1.72	0.98
<b>Volume (ml)</b>	178.79	175.51	175.01
<b>Concentration (mg/ml)</b>	.0033	.0098	.0056
<b>Absorption at 640 nm</b>	0.048	0.24	0.11
<b>Absorptivity <math>\alpha</math> (mL/mg<math>\times</math>meter)</b>	<b>1482</b>	<b>2434</b>	<b>1952</b>

### ***3.1.8 Optimal concentration***

With a definite absorptivity  $\alpha$  for each material, the final optimal concentration of each material, with an known absorption, could be calculated. Table 2 shows the tabulated final, optimal concentration for each material after decanting the supernatant from the suspensions following centrifugation. For all three materials, absorption values were taken at a wavelength of 800 nm from the highest absorption curves that had the optimal parameters of 30 minute continuous sonication tip method, 3 mg/ml surfactant, 3 mg/ml material, and 500 RPM centrifuge speed.

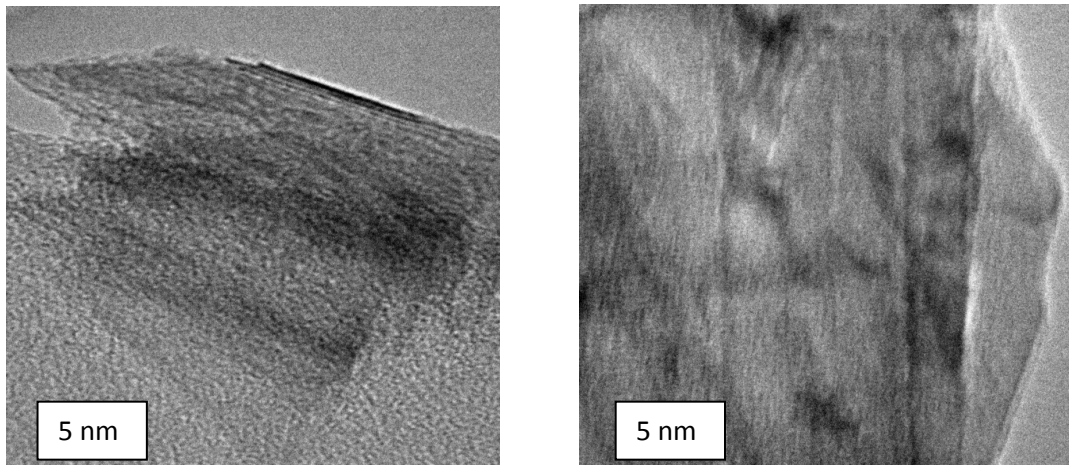
**Table 2.** Final optimal concentration of each material after the supernatant was removed from the suspensions.

<b>Material</b>	<b>WS<sub>2</sub></b>	<b>MoS<sub>2</sub></b>	<b>BN</b>
<b>Absorption at 800 nm</b>	0.46	0.91	0.26
<b>Absorptivity <math>\alpha</math> (mL/mg×meter)</b>	1482	2434	1952
<b>Concentration (mg/ml)</b>	<b>.031</b>	<b>.0098</b>	<b>.0056</b>

### **3.2 TEM results confirming layered flakes with hexagonal structures**

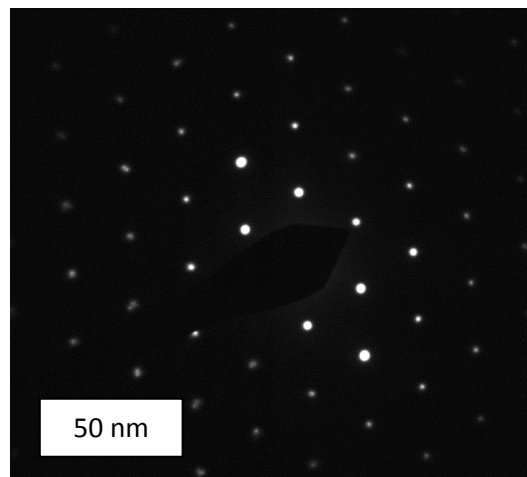
After the optimal suspensions with the highest absorption were found for all three materials, droplets of each suspension were casted onto circular meshed carbon films. TEM was performed on these films to 1) confirm that the exfoliation process was successful and 2) prove that these exfoliated inorganic materials had the layered, flaked, and symmetrically hexagonal characteristics needed to become potential materials for electronic applications.

TEM images in figure 9a show that MoS<sub>2</sub> had been successfully exfoliated. With overlapping fringes in stacked form, the exfoliated MoS<sub>2</sub> appeared in layers.



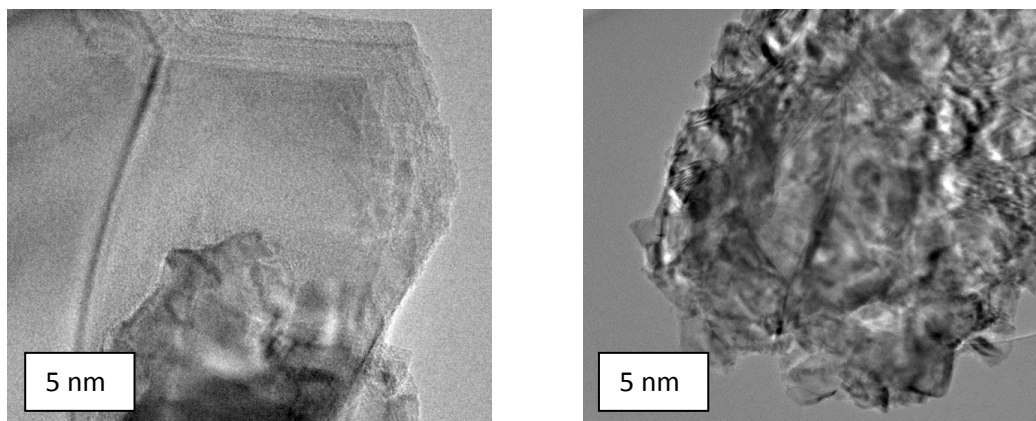
**Figure 9a.** TEM images showing the layered and flaked characteristics of exfoliated MoS<sub>2</sub>.

Figure 9b shows the diffraction pattern of exfoliated MoS<sub>2</sub>. The symmetric, orderly pattern resembles the basal hexagonal plane structure of graphene-like inorganic materials. This confirms that the exfoliation process did not change the structure of MoS<sub>2</sub>.



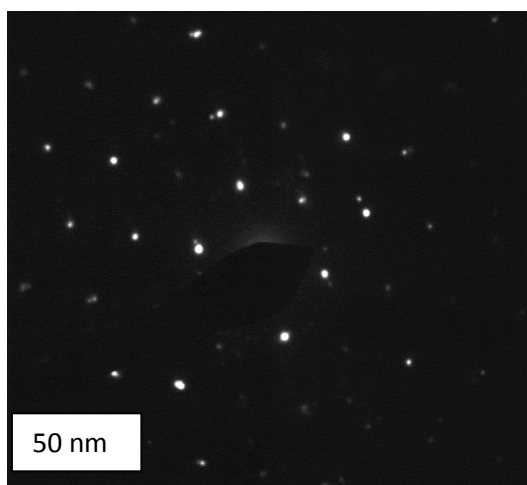
**Figure 9b.** Diffraction pattern reveals the hexagonal structure of exfoliated MoS<sub>2</sub>.

Similarly, TEM images in figure 10a show that WS<sub>2</sub> had also been successfully exfoliated. With many more overlapping fringes stacked together, the exfoliated WS<sub>2</sub> were certainly in layers.



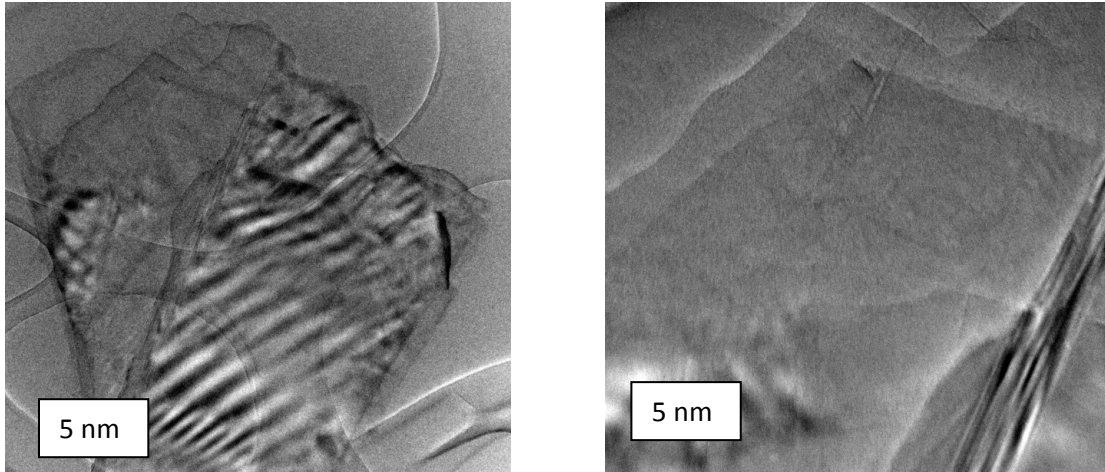
**Figures 10a.** TEM images showing the layered and flaked characteristics of exfoliated  $WS_2$ .

Figure 10b shows the diffraction pattern of exfoliated  $WS_2$ . Similar to the  $MoS_2$ , the symmetric, orderly pattern resembles the basal hexagonal plane structure of graphene-like inorganic materials. This also confirms that the exfoliation process did not change the structure of  $WS_2$ .



**Figure 10b.** Diffraction pattern reveals the hexagonal structure of exfoliated  $WS_2$ .

Finally, similar to those of  $MoS_2$  and  $WS_2$ , TEM images in **figure 11a** show that  $BN_2$  had been successfully exfoliated. With obvious overlapping fringes stacked together, the exfoliated  $BN_{also}$  appeared in layered form.



**Figures 11a.** TEM images showing the layered and flaked characteristics of exfoliated BN.

Figure 11b shows the diffraction pattern of exfoliated BN. The noticeable hexagonal pattern confirms that the exfoliation process did not change the structure of BN.

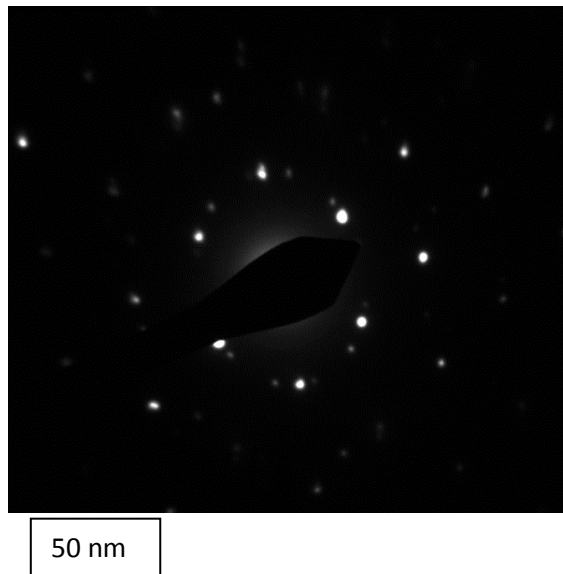


**Figure 11b.** Diffraction pattern reveals the hexagonal structure of exfoliated BN.

TEM analysis revealed that all of the three exfoliated materials were in layers and that their diffraction patterns resembled the hexagonal basis plane structure. The

symetric, layered, and flaked characteristics needed to develop inorganic nanofilm materials for potential electronic applications were indeed satisfied.

## 4. Conclusion

A carefully optimized method was developed to exfoliate inorganic graphene-like materials, such as molybdenum disulfide ( $\text{MoS}_2$ ), tungsten sulfide ( $\text{WS}_2$ ), and boron nitride (BN). When these three materials are successfully exfoliated into layers with hexagonal symmetric plane structures and casted onto carbon nanofilms, they can become potentially applicable electronic materials in sensing and energy storage devices.

The current study used a liquid-phase method to exfoliate the three inorganic materials ( $\text{MoS}_2$ ,  $\text{WS}_2$ , and BN). The method entails mixing different concentrations of each material with different concentrations of the surfactant sodium cholate hydrate ( $\text{C}_{24}\text{H}_{39}\text{NaO}_5 \cdot x\text{H}_2\text{O}$ ). to make suspensions samples. The suspensions are then dispersed through sonication and centrifuged. An optimization of the method was achieved sequentially to discover the optimal parameters (sonication method and duration, surfactant concentration, material concentration, and centrifuge speed) needed to generate suspensions with the highest concentration of each material. Through the Beer-Lambert's law, absorption is proportionally related to concentration in which a high absorption equated with a high concentration. Thus, the absorptions of all of the suspensions were measured by a UV-visible spectrometer, and the results were compared and analyzed to find out the optimal parameters.

The optimal parameters that led to the highest absorption, or concentration, for each of the three materials were: 3 mg/ml material concentration, 3 mg/ml surfactant concentration, 30-minute continuous tip sonication, and 1-hr 500 RPM centrifugation. Suspensions with the highest absorption were then casted onto carbon nanofilms. TEM was performed on these optimal suspensions to confirm the layered and hexagonal structure of each exfoliated material.

Optimizing the exfoliation process of inorganic materials is very important in the development of electronic and magnetic materials. These thin, layered, and hexagonal-structured graphene-like inorganic materials on nanofilms could be used as potentially cheap and efficient sensing and energy storage devices.

## **5. Future Study & Limitations**

There were limitations in this study. First, every parameter was only varied in a certain range. Future studies could expand the range of the parameter and see if other combinations yielded higher concentration of exfoliated materials. Such approach would be able to include more precise results and better error analysis. Also, in this study, only the optimization and exfoliation processes were carefully done and analyzed. In future studies, more experiments could be done on actually testing the electronic properties of these three materials to confirm that they would be good electronic materials. Lastly, the process of liquid-phase exfoliation could be done on more inorganic graphene-like materials.



## 6. References

- [1] D. Li. R. Kaner. *Science* 2008. Vol. 320, 1170.
- [2] G. Seifert. H. Terrones. M. Terrones. G. Jungnickel. *Physical Review Letters* 2000. 85, 1.
- [3] J. Coleman. M. Lotya. A.O'Neill. S.Bergin. *Science* 2011. 331, 568.
- [4] M. Lotya, Y. Hernandez, P. King, R. Smith, V. Nicolosi, *J. AM. CHEM* 2009, *No. 10*, 131.
- [5] M. Remskar, *Adv. Materials* 2004, *No. 17*, 16.
- [6] Y. Hernandez, V. Nicolosi, M. Lotya, F. Blighe. *Nature* 2008. 3, 563.